Accepted Manuscript

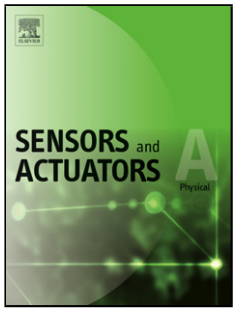

Title: Novel Dry Metal Electrode with Tilted Microstructure Fabricated with Laser Micromilling Process

Authors: Wei Zhou, Shaoyu Liu, Wei Liu, Chenying Zhang, Yaoyao Li, Wenjing Xu, Kwan San Hui

PII: S0924-4247(17)30319-9
DOI: http://dx.doi.org/doi:10.1016/j.sna.2017.07.028
Reference: SNA 10223

To appear in: *Sensors and Actuators A*

Received date: 22-2-2017
Revised date: 12-7-2017
Accepted date: 13-7-2017

Please cite this article as: Wei Zhou, Shaoyu Liu, Wei Liu, Chenying Zhang, Yaoyao Li, Wenjing Xu, Kwan San Hui, Novel Dry Metal Electrode with Tilted Microstructure Fabricated with Laser Micromilling Process, Sensors and Actuators: A Physicalhttp://dx.doi.org/10.1016/j.sna.2017.07.028

Novel Dry Metal Electrode with Tilted Microstructure Fabricated with Laser Micromilling Process

Wei Zhou [a] *, Shaoyu Liu [a], Wei Liu[a], Chenying Zhang [a], Yaoyao Li [a], Wenjing Xu [a], Kwan San Hui [b]

[a] Department of Mechanical & Electrical Engineering, Xiamen University, Xiamen 361005, China

[b] School of Mathematics, University of East Anglia, Norwich, NR4 7TJ, United Kingdom

Highlights

- > Dry metal electrodes with tilted microstructure arrays is fabricated. > Laser micromilling process of tilted microstructure arrays is discussed. > Effect of process parameters on surface microstructure arrays is investigated. > Optimized process parameters are obtained to fabricate tilted microstructure arrays. > Eelectrodes with tilted microstructures show lower impedance than vertical microstructures.

Abstract: A novel dry metal electrodes with tilted microstructure arrays was fabricated with laser micromilling process by adjusting the incident angle of the laser beam. After discussing the laser fabrication process for dry metal electrodes, the effects of the laser incident angle, width of unscanned area, laser output power, and scanning times on the shape and size of the microstructures are further discussed. Our experimental results show that the tilted angle of the surface microstructures of the dry metal electrodes depended on the laser incident angle. The heights of the surface microstructures of dry metal electrodes were greatly increased by increases of the laser output power and scanning times. Compared with vertical microstructure arrays, the developed dry metal electrodes with 60° tilted angle microstructure arrays demonstrated much lower impedances.

Keywords: Dry metal electrode; Laser micromilling; Surface microstructures; Impedance measurement

*Corresponding author. Tel.: 86-592-2188698; Fax: 86-592-2186383

E-mail address: weizhou@xmu.edu.cn (Wei Zhou).

1 Introduction

Over the last decade, the research on and applications of bioelectrical signals has been given increasing attention with the rapid development of modern medicine, neurology, and artificial intelligence. Bioelectrodes, which can be used to measure biological signals, have been widely used in modern clinical and biomedical measurements, including electrocardiograph (ECG), electroencephalogram (EEG), electromyography (EMG), gastric electrical activity, nerve potential, and electrical impedance imaging (EIT) measurements [1]. In the detecting process of biological electrical signals, a bioelectrode system, as a significant component of the measurement system, will come into direct contact with human skin, input a drive current, and receive a voltage signal for the purpose of exchanging and transmitting information. Because of the weak strengths of bioelectrical signals, there are strict conductivity requirements for bioelectrodes, which commonly use metal, silicon, or polymer as the base materials, covered by a conductive metal layer on the surface. Moreover, bioelectrodes, which come into direct contact with human skin, should be non-toxic and cannot cause allergic reactions [2]. Several bioelectrodes have been developed to meet the requirements for biological electrical signals measurement. Based on the structure style, bioelectrodes are divided into the traditional Ag/AgCl wet electrode, microneedle electrode, flexible

textile electrode, foam electrode and insulated dry electrode.

To fabricate the microstructure electrodes, the micromachining technology has been developed to fabricate microstructure arrays on silicon, metal, polymer, and glass, where the size of a single microstructure is usually 30–80 μm, with a length of more than 100 μm. Although most of the research has focused on an etching process to form microstructures on silicon [3–5], some researchers have developed some fabrication methods,such as traditional machining, electrochemical machining and 3D printing using the metal or other materials [6–13]. Ng et al. [6] developed a vacuum casting method to fabricate micro-spike dry EEG electrodes. These electrodes, which had a low impedance and stable performance, showed a good EEG measurement ability. Salvo *et al*. [7] developed a 3D printing method to fabricate a microneedle electrode, which was applied to EEG and ECG measurements and had a better performance than the traditional wet electrodes. Ruffini *et al.* [8] developed a novel electrode formed by carbon nanotubes. Because of its good ability to adhere to the surface of human skin, this electrode showed an accurate bioelectrical signal performance. Kitamura *et al.* [9-10] proposed an electrolytical method to fabricate electrodes using the steel wire. This method was simple, saved time, and allowed the shape of the microneedle structure to be controlled. Electrodes fabricated using this method had good performances as the traditional Ag/AgCl wet electrodes. Recently, seveal papers reported their work in developing novel dry electrodes with laser method. Laser processing, which is fast and accurate, has outstanding advantages in fabricating the microstructure[14-15]. For example, Gill *et al.* [16] developed a new method to fabricate miconeedle electrode, the

laser beam ablated the metal sheet and created the miconeedles in the plane of the sheet, then miconeedles was manually bent at 90° and electropolished, and the sizes and shapes of this electrodes can be controlled.

In this study, we proposed a laser micromilling fabrication method to make novel dry metal electrodes, which allows tilted microstructure arrays to be formed on the surface of the dry electrode by adjusting the incident angle of the laser beam. Based on the principle of the laser machining method, the effects of laser incident angle, width of unscanned area, laser output power, and scanning times on the shape and size of the microstructure were discussed in detail. Finally, impedance measurement of dry metal electrodes with tilted microstructure arrays was conducted and compared with vertical microstructure arrays.

2 Design, fabrication and impedance measurement of dry metal electrode

2.1 Structural design of dry metal electrode

A schematic diagram of a dry metal electrode with tilted microstructure array is shown in Fig.1. The metal dry electrode was composed of a metal electrode core, medical gauze, conductive silver glue, foam backing material, and shielding wire. The metal electrode core was made of red copper, which had good machinability and conductivity [17]. Laser micromilling was employed to fabricate the 6×6 microstructure arrays on the surface of metal electrode core with the size of 8×8 mm^2. After the laser micromilling process, platinum was sputtered on the core to improve the contact between the electrode core and human skin, which cloud improves the accuracy

of the biological electrical signal measurement. Moreover, a shielding wire was stuck to the metal electrode core using conductive silver glue and covered by a foam backing material. Then, the medical gauze was affixed to the back side, and the dry metal electrode was finally assembled. These surface microstructures are beneficial to improve the contact interface and increase the friction force between the electrode and skin, leading to a low contact impedance and better measurement stability.

2.2 Laser micromilling process

Fig. 2. shows the schematic diagram of the experimental setup for the laser micromilling process used for the dry metal bioelectrode. The system was composed of a fiber laser, collimator head, F-theta objective lens, computer controller, and machining platform [18]. In this study, a pulsed fiber laser (IPG) was used . The laser was set to produce 100 ns pulses with a 1064 nm central emission wavelength at a repetition rate of 20 kHz. The specifications of the characteristic parameters of the fiber laser system used are given in Table 1. The machining platform was composed of a linear motion device, rotating device, and fixture. The linear motion device was driven by a small stepper motor, which generated a reciprocating motion on the Z axis. A hinge was used to connect the linear motion device and rotating device, and the rotating device could rotate around the Y axis. The fixture was used to fix a copper plate. The incident angle of the laser beam could be controlled by changing the angle of the machining platform. In addition, laser processing parameters such as the unscanning area, laser output power, and scanning time could be adjusted through computer control.

One significant parameter of laser milling is the energy density (ED), which is

determined as follows:

$$ED = \frac{P_A}{V_{scan}\,\phi_{spot}} \quad (1)$$

where P_A is the output power of the laser source at a fixed frequency, V_{scan} is the scanning speed, and ϕ_{spot} is the focused diameter of the laser spot [19–21].

In this study, the threshold value of about 0.35 J/cm^2 can be experimentally derived for red copper matrial.When the laser output power was selected over 20 W and scanning speed below 1000mm/s, the red copper substrate can be fabricated.

2.3 Impedance measurement step

Fig. 3. shows the schematic diagram of impedance measurement of dry metal electrode. Two dry metal electrodes were placed on the forearm to measure the electrode–skin impedance, with a distance between the electrodes of 5 cm [22–23]. The dry metal electrodes did not require any treatment of the skin before the measurement [24–26]. Based on the two-electrode measurement principle, the same pair of electrodes could be used for the driving and measurement electrodes. The impedance analyzer (HIOKI Im3523 LCR Meter, Japan) was controlled by the Labview program through a USB interface. The computer sent a signal at a specific frequency to the impedance analyzer, which generated a sinusoidal current of 1 mA. Then, the impedance analyzer sent the current to the two electrodes on the forearm and measured their potentials. Finally, the impedance analyzer transmitted the impedance data to the computer through the USB interface, and the data was recorded and analyzed by Labview software. A frequency of 50 kHz was used by the impedance analyzer, and the working mode was the Z-R mode [27-28]. Short circuit and open circuit calibrations were

performed to improve the measurement accuracy before the impedance data was recorded.

3 Results and discussion

3.1 Formation process of tilted microstructure array

Laser processing is a thermal processing based on the photothermal effect. When a pulsed laser irradiates the base metal, it absorbs the laser beam energy, which causes the temperature of the metal to rapidly rise and exceed the evaporation temperature. The metal around the laser spot then melts even vaporizes at the high temperature, leading to material removal. The vaporized material will continue to interact with the laser beam, with some of the material becoming ionized and forming a plasma, which affect the further absorption of laser energy. Recasting is a normal phenomenon in the laser micromachining process. This phenomenon causes materials to transfer from the area that has been scanned by the laser to the area that has not been scanned [18]. With the help of this phenomenon, the recast layer stacking process can be controlled to form a microstructure array on the surface of the dry metal electrode.

As shown in Fig. 4a. to fabricate a dry metal electrode with a tilted microstructure array, the nested square machining path and loop multiple-pass reciprocating scanning strategies were used in this study. Fig. 4b. shows the schematic diagram of machining platform used to fabricate the dry metal electrodes. The incident angle (θ) of the laser beam directly affects the angle of the microstructures on the surface of the dry metal electrode. Fig. 4c. shows the effect of using a small scanning process for the substrate. As a result of gravity, the amount of recast metal below the molten pool was greater

than that above it. As the number of scans gradually increases, the laser energy is absorbed by the continuous irradiation of the laser. At this stage, the unscanned area was continually covered by the recast metal, as shown in Fig. 4d. Later, as the number of scans increases, a greater amount of surface material is heated to produce the metal steam pressure, which causes further external ejection of the liquid material to increase the depth and width of the scanning area, and a large quantity of metal is effectively removed during the laser micromilling process [29]. Finally, the recast metal is deposited and integrated with the unscanned area to form the cone microstructure array on the surface of the sample metal [30-31], as shown in Fig. 4e. Fig. 5. shows a typical scanning electron microscope (SEM) image of a tilted microstructure array on the surface of a dry metal electrode. It was verified that a tilted microstructure electrode could be successfully fabricated by controlling the incident angle of the laser beam.

3.2 Effects of process parameters on tilted microstructure array

3.2.1 Laser incident angle

Fig. 6. shows SEM images of dry metal electrodes with tilted microstructure arrays fabricated with different laser incident angles. The incident angle was set at 60°–90° by controlling the angle of the machining platform. The other machining parameters were fixed at a laser output power of 27 W, a scanning speed of 500 mm/s, 30 scanning times, and an unscanned area width of 100 μm. When the incident angle changes from 60° to 90°, the shape of the microstructures changes from a tilted style to a vertical style. Table 2 lists the measurement data of the tilted angle and height of microstructures fabricated with different laser incident angles. It can be observed from

the table that the error between the tilted angle of the microstructures and laser incident angle was within 2°. Furthermore, the height of the microstructures is also affected by the laser incident angle. When the laser incident angle was 60°, the height was found to reach a maximum value of 496 μm. However, the microstructure array could not be fabricated with a small laser incident angle. Therefore, we recommend 60° laser incident angle to produce the microstructure array on the surface of dry metal electrodes with much better quality.

3.2.2 Width of unscanned area

The machining path is one of the most important parameters influencing the laser micromilling process. In this experiment, a nested square machining path was selected, and the inner square was the unscanned area, as shown in Fig. 4. Widths of 60 μm, 80 μm, 100 μm, and 120 μm were selected for the unscanned area under the predetermined conditions of a laser output power of 27 W, a scanning speed of 500 mm/s, 30 scanning times, and a 60° laser incident angle. When the width was set at 60 μm, it was obvious that an microstructure array was formed on the surface of the sample metal, as shown in Fig. 7a. This was mainly because the small unscanned area led to a small area for recasting, but the small recast area could not hold most of the molten and vaporized metal. When the width was increased to 120 μm, the unscanned area was too large to be covered by the recast metal, which led to ladder structures. However, when a width of 80–100 μm was selected, the cone microstructure arrays were formed, which means the recast metal exactly covered the unscanned area, as shown in Fig. 7b. and c.

Fig. 8. shows the influence of the unscanned area width on the height and bottom width of tilted microstructurethe of dry metal electrode. It can be seen that the width of the unscanned area has a significant influence on the bottom width of the microstructures. When the width of the unscanned area was increased from 60 μm to 120 μm, the bottom width of the microstructures increased from 151 μm to 379 μm. The height of the microstructures gradually increases when the width of the unscanned area increases from 60 μm to 100 μm, but when the width increases to 120 μm, the height decreases. These changes were attributed to the difficulty of covering a large unscanned area with the recast metal material and the fact that a small unscanned area could not hold most of the recast metal material. Thus, in both cases, the cone microstructure array could not be formed. Therefore, 80–100 μm was the optimized width for the unscanned area.

3.2.3 Laser output power

The laser output power is one of the significant parameters in the micromilling process. Laser output power values of 21 W, 24 W, 27 W, and 30 W were selected under the predetermined conditions of a scanning speed of 500 mm/s, 30 scanning times, an unscanned area width of 100 μm, and a 60° laser incident angle. The effects of the laser output power on the shape and size of the microstructures were studied based on the SEM images. When the laser output power was 21 W, the surface microstructures could not be effectively fabricated because the low laser energy made it difficult to fully achieve the surface evaporation and melting process of the surface metal material, which led to a low material removal rate, as shown in Fig. 9a.

However, when the laser output power was increased to more than 24 W, the material melting and evaporation phenomena become much easier to induce because of the higher temperature[27]. Finally, the surface material was removed to produce the surface microstructures, as shown in Fig. 9b. to d. The influence of the laser output power on height and bottom width of tilted microstructures of dry metal electrode is shown in Fig.10. When the laser output power was increased from 21 W to 30 W, the bottom width increases from 229 μm to 359 μm, and the height increases from 248 μm to 480 μm. It is worth noting that the laser output power has a greater influence on the height of the microstructures than on the bottom width. This was attributed to the fact that the influence of the laser output power on the depth of the melting zone was greater than that on the width.

3.2.4 Scanning times

The scanning times, which determined the quality of the structure, also needed to be adjusted in the laser micromilling process. SEM images of tilted microstructures produced using different scanning times are shown in Fig. 11. Where the predetermined conditions were a laser output power value of 27 W, a scanning speed of 500 mm/s, an unscanned area width of 100 μm, and a laser incident angle of 60°. When the scanning times were less than 10 times, it was difficult to form the top of the microstructures, and the total height was low, as a result of the low material removal rate, as shown in Fig. 11a. When the scanning times were increased to 20 times, the cone microstructure array were gradually formed, as shown in Fig. 11b. Finally, when more than 30 scanning times were used, the cone microstructure array

were successfully fabricated, as shown in Fig. 11c. and d. However, the scanning times had a greater effect on the height of the microstructures than on their width, which can be seen in Fig. 12. When the scanning times were increased from 10 times to 50 times, the height of the microstructures increased from 126 μm to 480 μm, whereas the width increased from 160 μm to 314 μm. Therefore, to obtain dry metal electrodes with a tilted surface microstructure array, the scan times should be greater than 30.

3.3 Impedance measurement

Fig. 13. shows the impedance measured value using dry metal electrodes with different tilted degree microstructure array and without microstructure array. Under the same measurement conditions, the dry metal electrodes with tilted degree microstructure array had lower average impedance values comparing with the electrodes without microstructure array. Furthermore, the dry metal electrodes with the 60° tilted microstructure array had lower average impedance values than those with the vertical microstructures (less about 18 Ω), as show in Fig. 13a. Fig. 13b. shows the impedance measurements over a period of 20 min. The impedance measured by the dry metal electrodes with 60° tilted microstructures presented small fluctuations in the first 15 min, and then gradually became stable, reaching a value that was lower than that of the electrodes with the vertical microstructures (90°). This can be attributed to the fact that the dry metal electrodes with the tilted microstructures fit more tightly than those with the vertical microstructures. However, the tilted microstructures may have needed more time to become joined to the skin, which led to a slightly longer settling time.

Therefore, the dry metal electrodes with the tilted microstructures have an advantage in long-term impedance measurement compared with those with vertical microstructures.

4 Conclusions

Tilted microstructure arrays could be fabricated with laser micromilling process on the surface of dry metal electrodes by adjusting the incident angle of the laser beam. The influence of the laser incident angle, unscanning area width, laser output power and scanning times on the formation of the microstructure was discussed. In the laser micromilling process, the tilted angle of the surface microstructures of the dry metal electrodes depended on the laser incident angle, and the error between the tilted angle of microstructures and laser incident angle was within 2°. The unscanned area affected the fabrication of the tilted microstructures, where a width of 80–100 μm was found to be the most suitable for the unscanned area. The height of the microstructures was greatly increased by increasing the laser output power and scanning times. However, a laser incident angle 60°, a laser output power of 27 W, 30 scanning times, and an unscanned area width of 100 μm were the most suitable and economic machining parameters for fabricating the dry metal electrodes with 60° tilted microstructures. In addition, the dry metal electrodes with tilted microstructures had much smaller impedance in a bioelectrical measurement compared with those with vertical microstructures. Therefore, the developed dry metal electrodes with tilted microstructures, which are economic and convenient, have promising applications in bioelectrical measurement.

Acknowledgments

This work was supported by the National Natural Science Foundation of China (Project No. 51475397) and the Fundamental Research Funds for Central Universities, Xiamen University (Project No. 20720160079). In addition, the supports from Open Fund of Shanghai Key Laboratory of Digital Manufacture for Thin-Walled Structures (No.2015004) and the Collaborative Innovation Center of High-End Equipment

Wei Zhou received received his Ph.D. degrees in mechanical engineering from South China University of Technology, Guangzhou, China,in 2010. From 2010 to 2012, he was a postdoc researcher at Sun Yat-sen University. He was appointed as an associate professor in mechanical & electrical engineering of Xiamen University from Dec 2012 - Juy 2016. Now he is an professor at Xiamen University. His current research interests focus on design, fabrication and performance evaluation of biomedical device.

Shaoyu Liu starts to work toward the Ph.D. degree in mechanical engineering at Xiamen University 2014. His research interests are in microfabrication technology of biomedical device.

Wei liu starts to work toward the Ph.D. degree in mechanical engineering at Xiamen University since 2014. Her research interests are in the area of measurement methods of different bioelectrodes.

Chenying Zhang starts to work toward the Ph.D. degree in mechanical engineering at Xiamen University since 2014. His research interests are in the area of the optimization of fabrication process of bioelectrodes.

Yaoyao Li starts to work toward the M.D. degree in mechanical engineering at Xiamen University since 2017. His research interests are in the area of the design and fabrication method of bioelectrodes.

Wenjing Xu starts to work toward the M.D. degree in mechanical engineering at Xiamen University since 2014. Her research interests are in the area of modeling and simulation of microfabrication process of bioelectrode.

Kwan San Hui received his PhD degree in the department of mechanical engineering at the Hong Kong University of Science and Technology in 2008. He was appointed as

a lecturer in department of systems engineering and engineering management of City University of Hong Kong, Hong Kong from Aug 2008 - Feb 2012. In Mar 2013, he worked as an Assistant Professor in Department of Mechanical Engineering at Hanyang University, South Korea. In Sep 2016, he was appointed as a Lecturer in Mechanical Engineering, School of Mathematics, Faculty of Science, University of East Anglia, UK. He has extensive research experience in material science, catalysis, air/water pollution control, and energy storage.

Manufacturing in Fu Jian are also acknowledged.

References

[1] S. Enrique, H. Marcelo, Insulating electrodes: A review on biopotential front ends for dielectric skin-electrode interfaces, Physiol. Meas. 31(2010) 183-198.

[2] L. S. Hsu, S.W. Tung, C.H. Kuo, Y. J. Yang, Developing barbed microtip-based electrode arrays for biopotential measurement, Sensors. 14 (2014) 12370–12386.

[3] S.J. Lee, H.S. Hoon, X. Xuan, J.Y. Park, A patch type non-enzymatic biosensor based on 3D SUS micro-needle electrode array for minimally invasive continuous glucose monitoring, Sens. Actuators, B. 222 (2016) 1144–1151.

[4] P. Griss, P. Enoksson, H. K. Tolvanen-Laakso, P. Merilainen, S. Ollmar, G. Stemme, Micromachined electrodes for biopotential measurements, J. Microelectromech. S. 10 (2001) 10–16.

[5] P. Griss, P. Enoksson, H. K. Tolvanen-Laakso, P. Merilainen, G. Stemme, Characterization of micromachined spiked biopotential electrodes, IEEE T. Bio-med. Eng. 49 (2002) 597–604.

[6] W.C. Ng, H.L. Seet, K.S. Lee, N. Ning, W.X. Tai, M. Sutedia, J.Y.H. Fuh, X.P. Li, Micro-spike EEG electrode and the vacuum-casting technology for mass production, J. Mater. Process. Technol. 209(2009) 4434–4438.

[7] P. Salvo, R. Raedt, E. Carrette, D. Schaubroeck, J. Vanfleteren, L. Cardon, A 3D printed dry electrode for ECG EEG recording, Sens. Actuators, A. 174 (2012) 96–102.

[8] G. Ruffini, S. Dunne, E. Farres, J. Marco-Pallares, C. Ray, E. Mendoza, R. Silva, C. Grau, A dry electrophysiology electrode using CNT arrays, Sens. Actuators, A. 132 (2006) 34–41.

[9] N. Kitamura, J. Chim, N. Miki, Electrotactile display using microfabricated micro-needle array, J. Micromech. Microeng. 25 (2015) 025016.

[10] M. Tezuka, N. Kitamura, K. Tanaka, N. Miki, Presentation of various tactile sensations using micro-needle electrotactile display, PLoS One. 11 (2016) 0148410.

[11] R. Prehn, M. Cortina-Puig, F.X. Mun, A non-enzymatic glucose sensor based on the use of gold micropillar array electrodes, J. Electrochem. Soc. 159 (2012) 134–139.

[12] Y. Wang, W.H. Pei, K. Guo, Q. Gui, X.Q. Li, H.D. Chen, J.H. Yang, Dry electrode for the measurement of biopotential signals, Sci. China Inform. Sci. 54 (2011) 2435–2442.

[13] C.F. Pan, K.Y. Chen, L.L. Jiang, Z.P. Chen, L. Ren, L. Liang, W. Yuan, Magnetization-induced self-assembly method: Micro-needle array fabrication, J. Mater. Process. Technol. 227 (2016) 251–258.

[14] M. Tang, V. Shim, Z. Y. Pan, Y. S. Choo, M. H. Hong, Laser ablation of metal substrates for super-hydrophobic effect, J. Laser Micro. Nanoen. 6 (2011) 6-9.

[15] Y. C. Guan, W. Zhou, Z. L. Li, H. Y. Zheng, G. C. Lim, M. H. Hong, Femtosecond laser-induced ripple structures on magnesium. Appl. Phys. A Mater. Sci. Process. 115 (2014) 13-18.

[16] H. S. Gill, M.R. Prausnitz, Coated microneedles for transdermal delivery, J. Control. Release. 117(2007) 227-237.

[17] W. Zhou, R. Song, X.L. Pan, Y.J. Peng, X.Y. Qi, J.H. Peng, K.S. Hui, K.N. Hui, Fabrication and impedance measurement of novel metal dry bioelectrode, Sens. Actuators A. 201 (2013) 127–133.

[18] S.W. Lee, H.S. Shin, C.N. Chu, Fabrication of micro-pin array with high aspect ratio on stainless steel using nanosecond laser beam machining, Appl. Surf. Sci. 264 (2013) 653–663.

[19] X. Wang, L.Y. Li, Z.B. Shen, C.F. Sha, Experimental investigation on: Laser shock micro-forming process using the mask and flexible pad, Opt. Lasers Eng. 88 (2017) 102–110.

[20] L. M. Vilhena, M. Sedlacek, Surface texturing by pulsed Nd:YAG laser, Tribol. Int. 42 (2009) 1496–1504.

[21] M. Miyagi, X.D. Zhang, Y. Kawahito, S. Katayama, Surface void suppression for pure copper by high-speed laser scanner welding, J. Mater. Process. Technol. 240 (2017) 52–59.

[22] A. K. Srivastava, B. Bhartia, K. Mukhopadhyay, A. Sharma, Long term biopotential recording by body conformable photolithography fabricated low cost polymeric microneedle arrays, Sens. Actuators A. 236 (2015) 164–172.

[23] L. Chinteng, L. Lunde, L. Yuhang, B.S. Lin, J.Y. Chang, Novel dry polymer foam electrodes for long-term EEG measurement, IEEE T. Bio-med. Eng. 58(2011) 1200–1207.

[24] T. Gratieri, I. Alberti, M. Lapteva, Y.N. Kalia, Next generation intra- and transdermal therapeutic systems: Using non- and minimally-invasive technologies to increase drug delivery into and across the skin, Eur. J. Pharm. Sci. 50 (2013) 609–622.

[25] J. H. Park, S. O. Choi, S. Seo, Y. Bin Choy, M. R. Prausnitz, A microneedle roller for transdermal drug delivery, Eur. J. Pharm. Biopharm. 76 (2010) 282–289.

[26] S. A. Ranamukhaarachchi, T. Schneider, Development and Validation of an Artificial Mechanical Skin Model for the Study of Interactions between Skin and Microneedles Macromol. Mater. Eng. 301(2016) 306−314.

[27] M. Arai1, Y. Nishinaka, Electroencephalogram measurement using polymer-based dry microneedle electrode, Jpn. J. Appl. Phys. 6 (2015) 06FP14.

[28] B. H. Brown, Medical impedance tomography and process impedance tomography: a brief review. Meas. Sci. Technol. 12(2001) 991–996.

[29] J. Ho, C. Grigoropoulos, J. Humphrey, Computational study of heat-transfer and gas-dynamics in the pulsed-laser evaporation of metals, J. Appl. Phys. 78(1995) 4696-4709.

[30] L. M. Vilhena, M. Sedlacek, Surface texturing by pulsed Nd:YAG laser, Tribol. Int. 42 (2009) 1496–1504.

[31] D. Du, Y.F. He, B. Sui, L.J. Xiong, H. Zhang, Laser texturing of rollers by pulsed

Nd:YAG laser, J. Mater. Process. Technol. 161(2005) 456–61.

Figure captions

Fig.1 Schematic diagram of dry metal electrode with tilted microstructure array：1-metal electrode core, 2-shielding wire, 3-conductive silver glue, 4-foam backing material, and 5- medical gauze

Fig.2 Schematic diagram of the experimental setup for the laser micromilling process used for the dry metal bioelectrode.

Fig.3 Schematic diagram of impedance measurement of dry metal electrode

Fig.4 Schematic diagram of forming process of tilted microstructure array on the dry metal electrode

Fig.5 Typical SEM image of a tilted microstructure array on the surface of a dry metal electrode

Fig.6 SEM images of dry metal electrodes with tilted microstructure arrays fabricated with different laser incident angles：(a) 60°, (b) 70°, (c) 80°, and (d) 90°（Vertical incident）

Fig.7 SEM images of dry metal electrodes with tilted microstructure arrays fabricated with different unscanned area widths：(a) 60 μm, (b) 80 μm, (c) 100 μm, and (d) 120 μm

Fig.8 influence of the unscanned area width on the height and bottom width of tilted microstructurethe of dry metal electrode

Fig.9 SEM images of dry metal electrodes with tilted microstructure arrays fabricated with different laser output power values: (a) 21 W, (b) 24 W, (c) 27 W, and (d) 30 W

Fig.10 Influence of laser output power on height and bottom width of tilted microstructures of dry metal electrode

Fig.11 SEM images of dry metal electrodes with tilted microstructure arrays fabricated with different scanning times：(a) 10, (b) 20, (c) 30 and (d) 50

Fig.12 Influence of scanning times on height and bottom width of tilted microstructures of dry metal electrode

Fig.13 Impedance measured value using dry metal electrodes with different tilted degree microstructure array and without microstructure array

Table captions

Table 1 Specifications of characteristic parameters of fiber laser system

Table 2 Tilted angle and height of microstructures fabricated with different laser incident angles

Figr-1

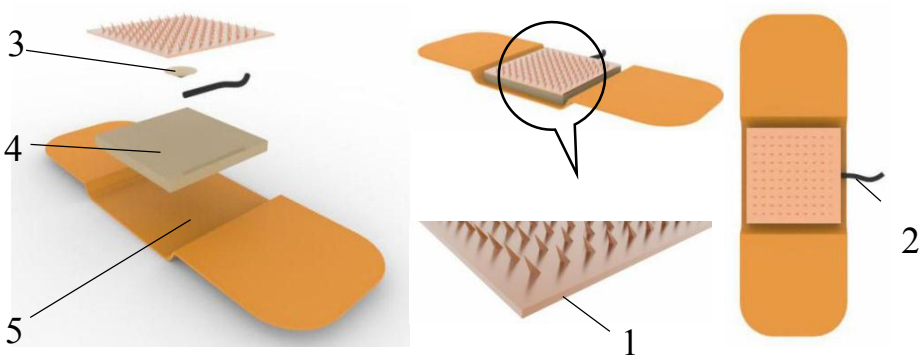

Fig.1

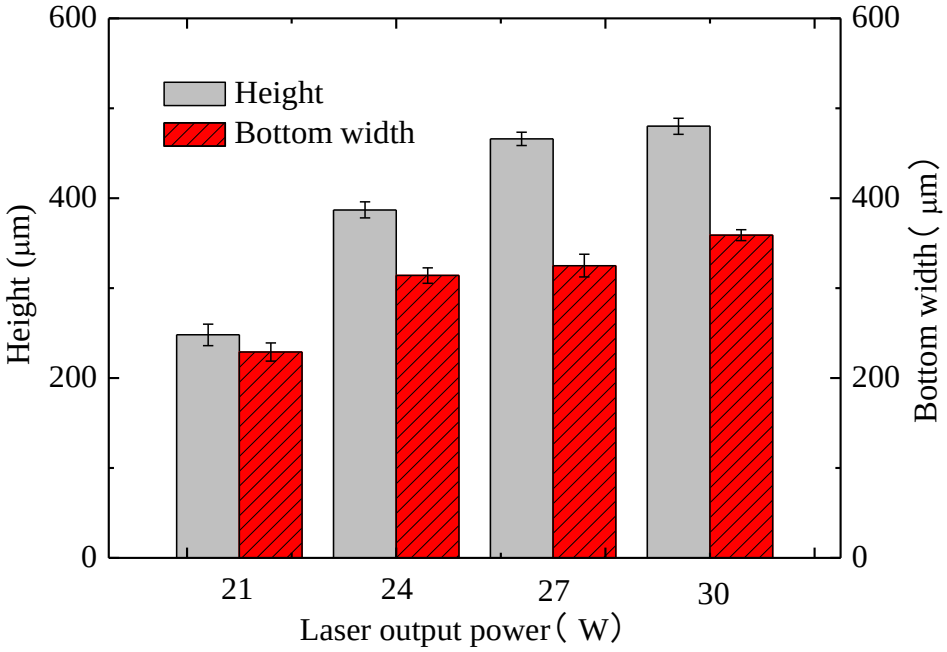

Figr-2

Fig.10

Figr-3

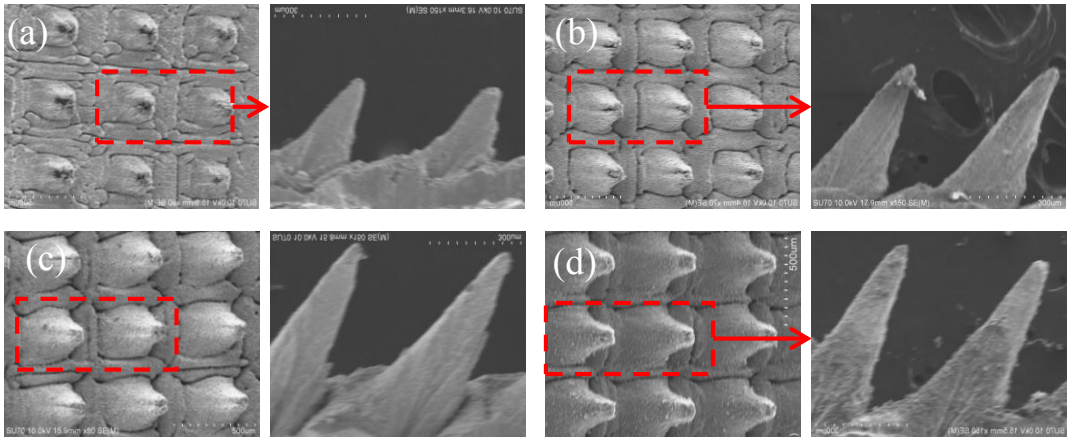

Fig.11

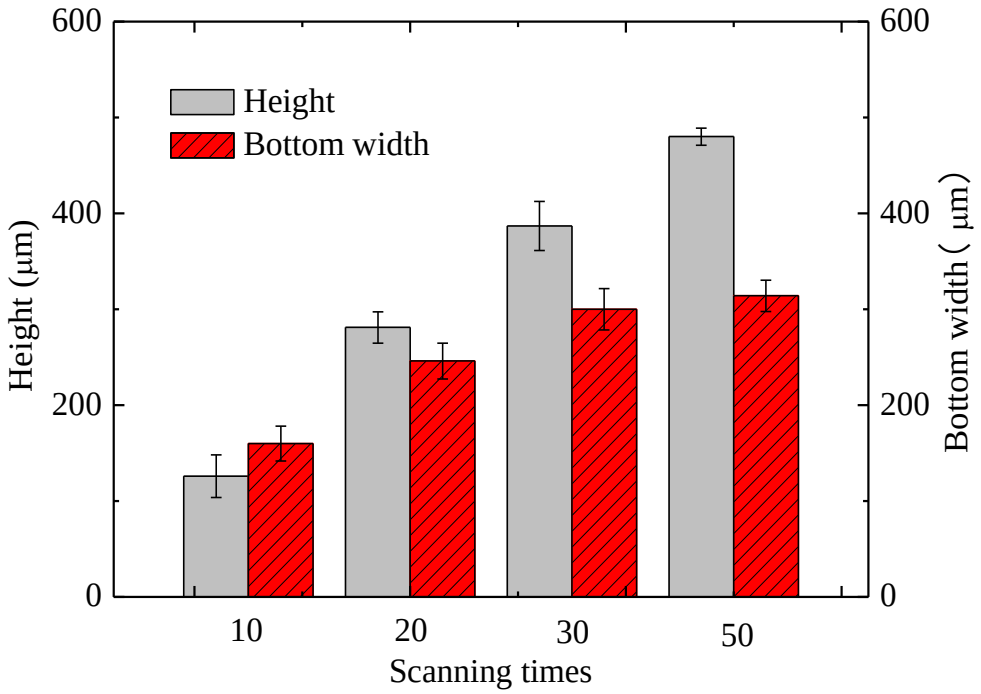

Figr-4

Fig.12

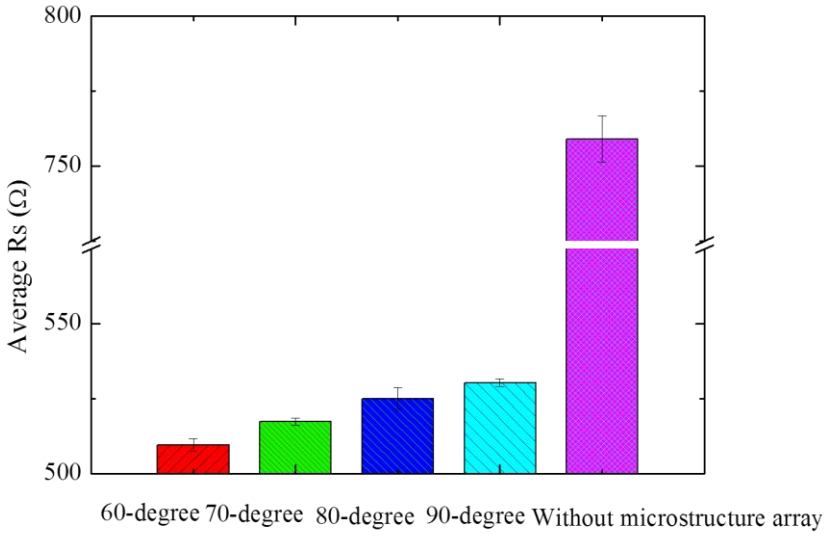

(a) Average impedance over 20

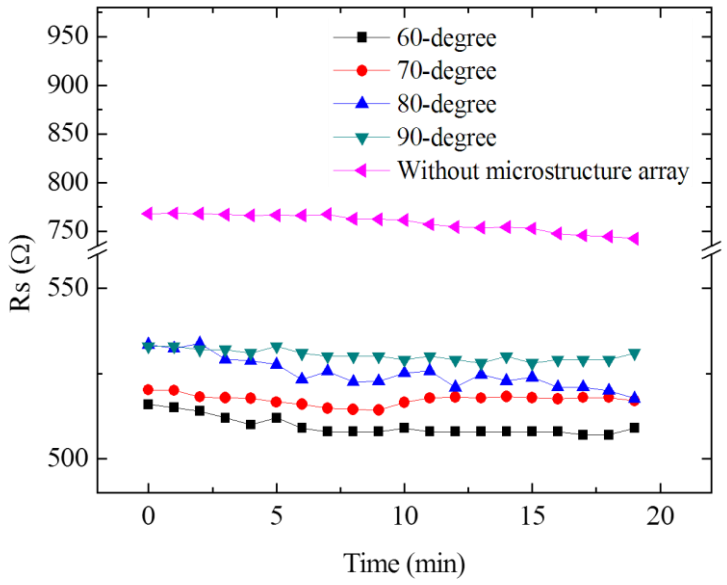

(b) Impedance measurement over 20 min

Figr-5

Fig.13

Figr-6

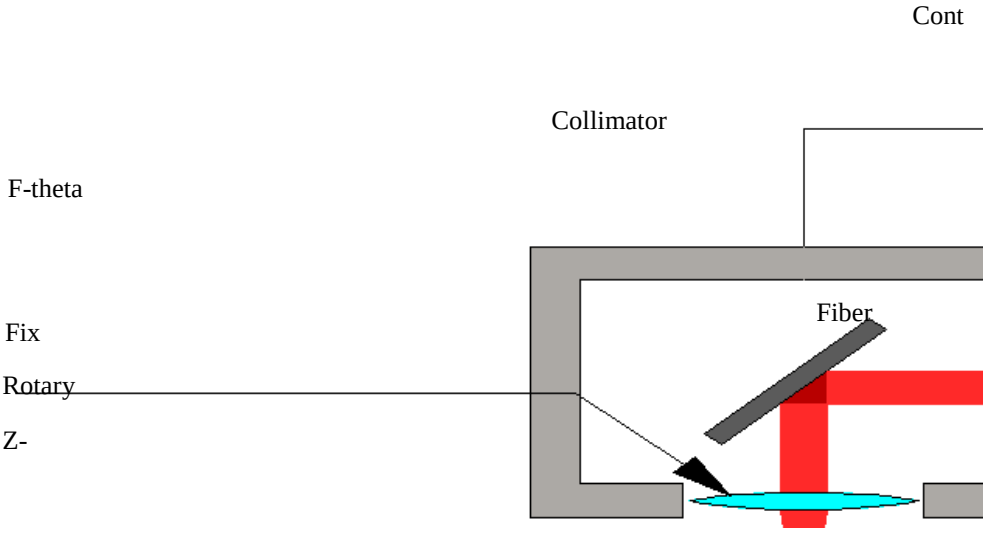

Fig.2

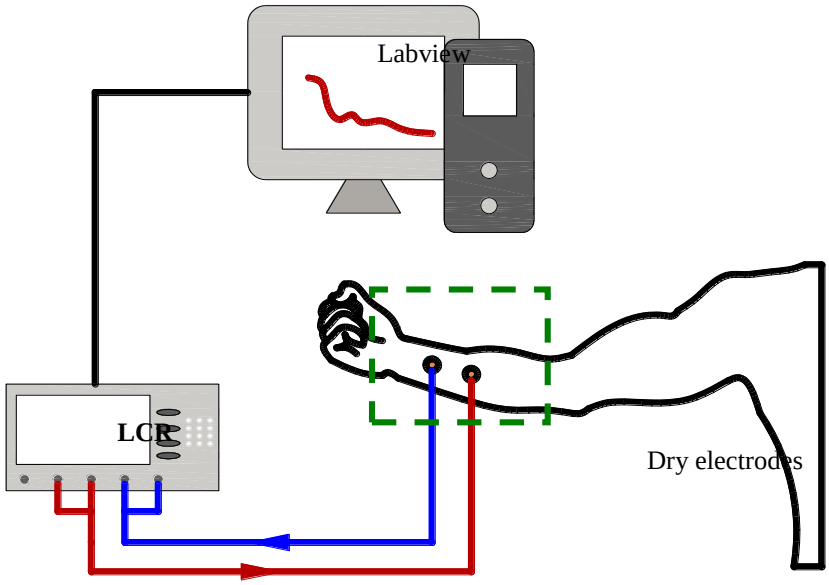

Figr-7

Fig.3

Figr-8

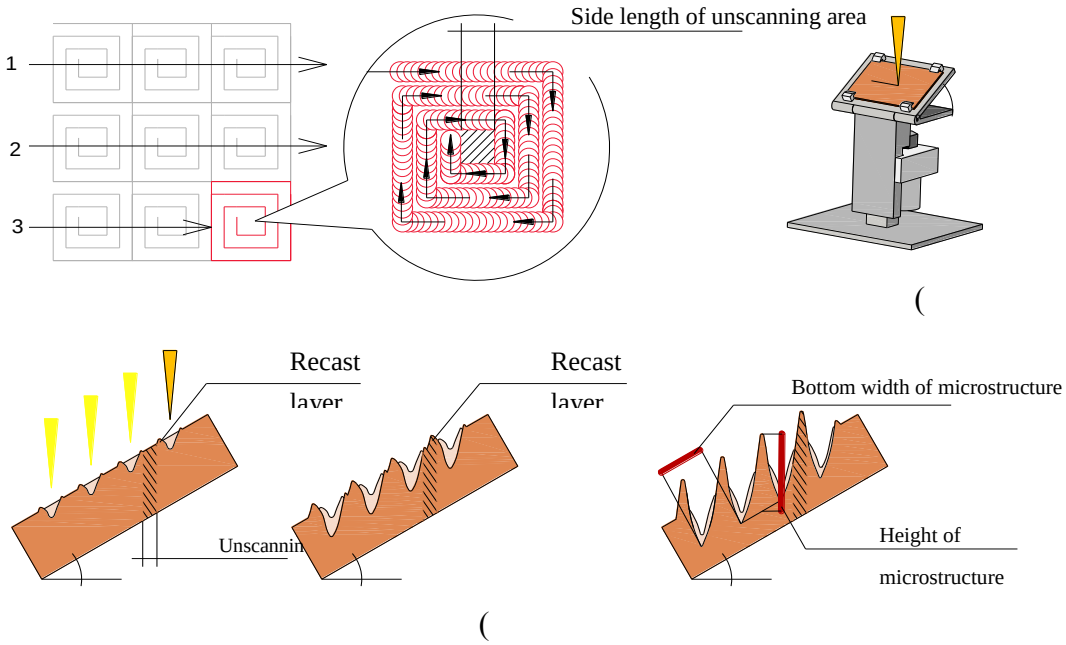

Fig.4

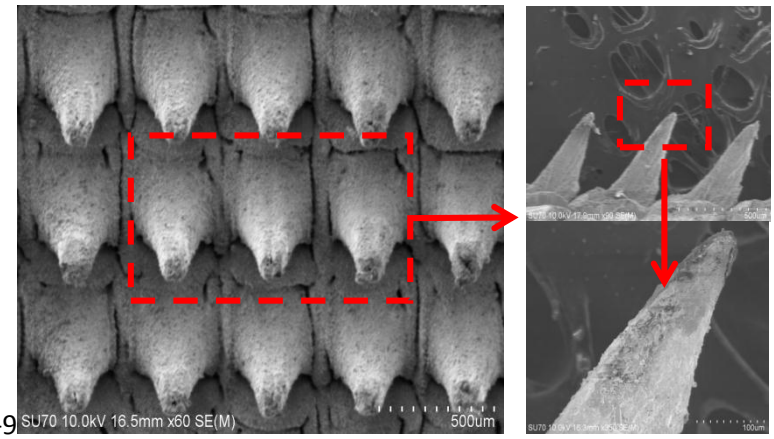

Figr-9

Fig.5

Figr-10

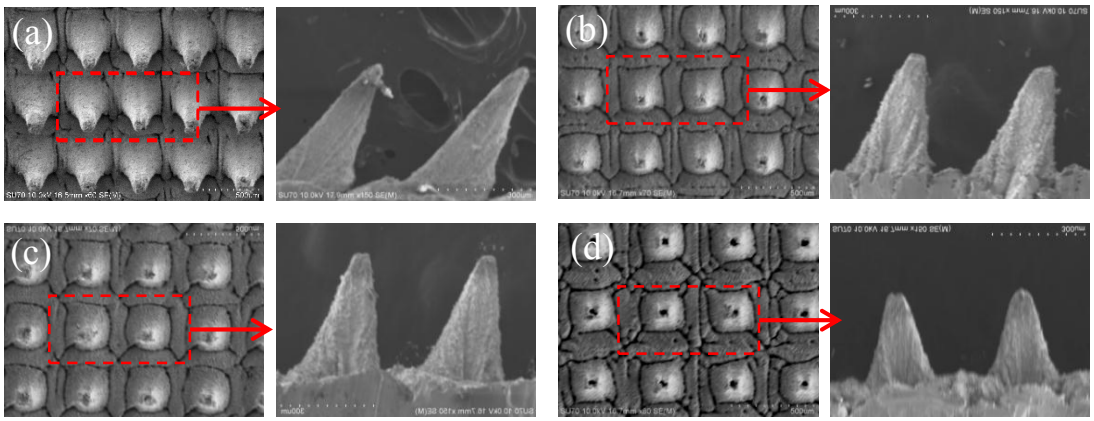

Fig.6

Figr-11

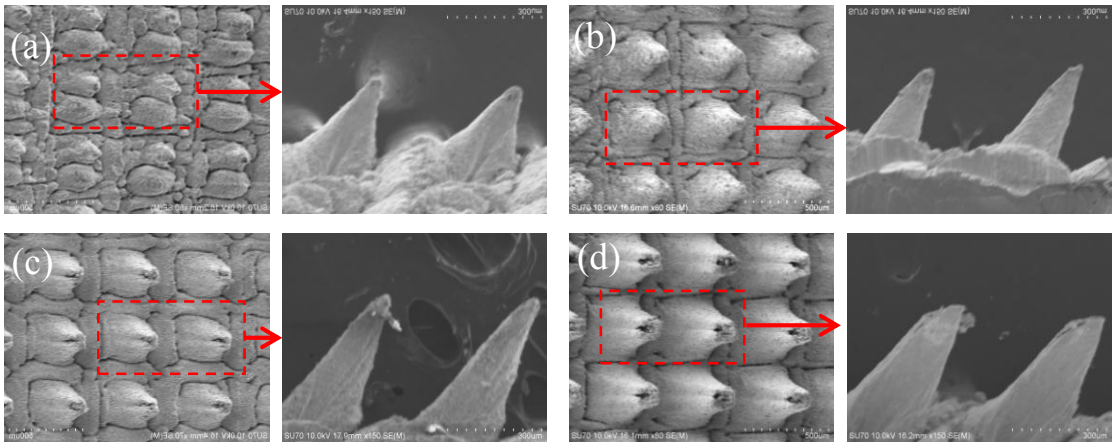

Fig.7

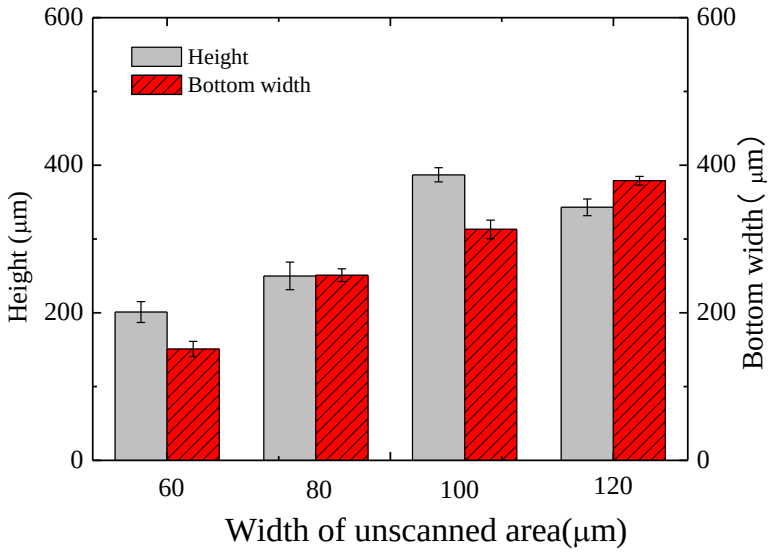

Figr-12

Fig. 8

Figr-13

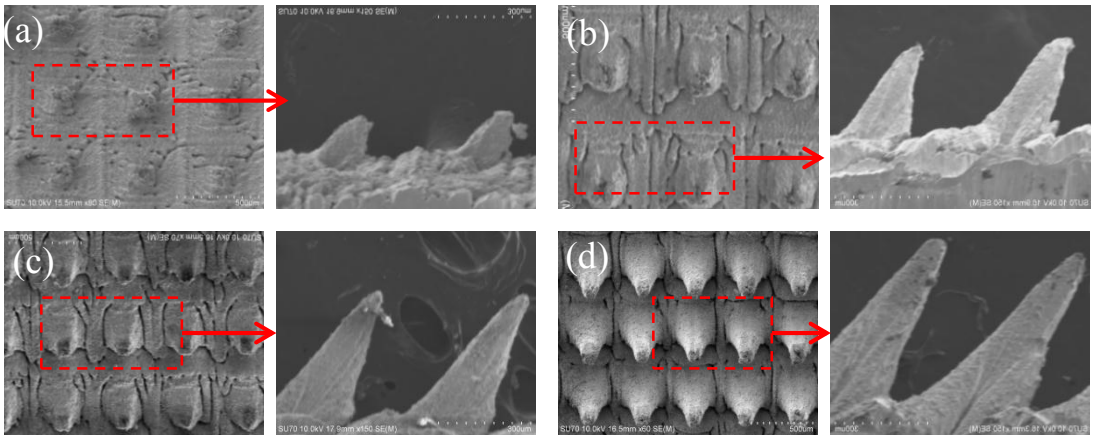

Fig.9

Table 1

Characteristic	Parameter range	Assumed parameter	Unit
Wavelength	1055~1070	1064	nm
Nominal average output power	29~31	30	W
Pulse duration	90~120	100	ns
Repetition rate	20~200	20	kHz
Beam quality (M^2)	<1.1	1	
Incident beam diameter	6~9	7	mm
Focused diameter	24.3~37.3	31.5	μm

Table 2

Laser incident angle	Height of microstructure (μm)	Titled angle of microstructure
60°	459.9	58.3°
70°	395.5	71.8°
80°	371.2	78.2°
90°	320.6	89.5°